Two-dimensional Numerical Simulation of Microwave Imaging Reflectometry

Zhongbing Shi[1)], Yoshio Nagayama[2)], Daisuke Kuwahara[3)], Tomokazu Yoshinaga[2)], Masaharu Sugito[2)], Soichiro Yamaguchi[4)]

[1)] *The Graduate University for Advanced Studies, Toki 509-5292, Japan*
[2)] *National Institute for Fusion Science, Toki 509-5292, Japan*
[3)] *Department of Energy Science, Tokyo Institute of Technology, Tokyo 152-8550, Japan*
[4)] *Kansai University, Suita 564-8680, Japan*

(Received: 3 September 2008 / Accepted: 7 November 2008)

This work describes a numerical study of the two dimensional turbulent fluctuations in microwave imaging reflectometry (MIR) system. The numerical results show that the fluctuations of the cutoff surface can be obtained from the phase of the reflected waves when these are collected with a wide aperture optical lens system, which is used to form an image of the cutoff onto the detector surface. A laboratory arrangement of the MIR system is made. The preliminary tests show that the MIR system works well at the in-focus condition when the fluctuation amplitude is much smaller than the wavelength of the launching wave. However, the reflected signals are distorted at strong fluctuations. The relationships between the fluctuation amplitude and the wavenumber of the fluctuation which may cause the distortions of the reflected signals, are discussed.

Keywords: Microwave imaging Reflectometry (MIR), density fluctuation

1. Introduction

Microwave reflectometry is a powerful tool to measure the plasma density profile and density fluctuation [1–3]. In a reflectometry system, the microwave illuminates the plasma, and the wave is reflected by the cutoff layer in the plasma. The phase difference between the incident wave and the reflected wave is detected. The reflected wave is mainly modified by the density fluctuations close to the cutoff region, and the phase fluctuation is proportional to the density fluctuation as $\phi \propto L_n \tilde{n}/n$, where $L_n = n/(dn/dr)_{r=r_c}$ is the reverse density gradient length at the cutoff surface. The wave propagation is well understood in a one-dimensional (1D) reflectometer system [1]. However, in the two-dimensional (2D) and three-dimensional (3D) configurations the complicated interference pattern appears on the detection plane, because the reflected wave propagates in different directions. Therefore, it is very difficult to extract any useful information from the fluctuations [1, 4–6].

To correct the disturbed wave front, the optical imaging technique is used in the reflectometry, named as microwave imaging refelctometry (MIR) [1,4]. This diagnostic system uses the wide aperture optics to form an image of the reflected surface onto a 2D detector array located at the image plane. The time evolutions of 2D pictures of density fluctuation at the cutoff surface are captured, just like a movie. The feasibilities of MIR for turbulence measurement have been investigated in theories and experiments [1, 4, 7–10] intensively. So far, the MIR diagnostics are under development in several fusion devices, such as LHD, DIII-D and ASDEX-U [4,7]. The further understanding of the received signals is very important to develop the next generation of MIR system. Although the encouraging initial results have been obtained in TEXTOR and LHD, there remain many issues [4, 7, 11], such as the fringe jump, the antenna array and receiver array. Among them, the optical aberration is one of the biggest issues. Therefore, the optical lens must be considered in the simulation.

Simulations have been performed at the standard reflectometry without imaging optics [6,8,12]. In this work, the numerical simulation model based on the Huygens-Fresnel equation is used to simulate the wave propagation in a microwave imaging system. The optical lens is considered in this model. A laboratory arrangement of the MIR system is made. The experimental results show that the MIR system works well at the in-focus condition when the fluctuation amplitude is much smaller than the wavelength of the launching wave. However, the reflected signals are distorted at strong fluctuations. Both the simulation and the experiments show that the distortions of the reflected signals depend on not only the fluctuation amplitude but also the wavenumber of the fluctuation. Their relationships are discussed by the geometrical approximation.

Section 2 contains a description of the numerical simulation based on the Huygens-Fresnel equation, which is used for the propagation of the reflected signals. The simulation results in the case of different amplitude and the phase fluctuations are shown. The

author's e-mail: shi.zhongbing@nifs.ac.jp

arrangement of the MIR is described in section 3. The weak and strong fluctuations obtained from MIR system are compared and explained. The summary and discussions are given in section 4.

2. Numerical simulation

2.1 Model

The electric field in all space can be calculated from the Maxwell equation. It is used in the reflectometer model for the propagation of reflected signals. In this simulation, we assume the wave is only reflected at the cutoff surface in vacuum. The full wave equation can be solved by means of Fourier method, given as follows [12]:

$$E(x,z) = \frac{1}{2\pi}\int_{-\infty}^{\infty} E_z(k_z) e^{i(k_z z + x\sqrt{k_0^2 - k_z^2})} dk_z \quad (1)$$

$$E_z(k_z) = \int_{-\infty}^{\infty} E_0(z) e^{-ik_z z} dz \quad (2)$$

where k_0 is the wavenumber of the incident microwave, $E_0(z)$ is the distribution of the incident microwave at position x_0, given as:

$$E_0(z) = E_{x_0}(z) e^{-z^2/w^2} e^{ik_0 z^2/\rho} e^{i\phi} \quad (3)$$

here, $E_{x_0}(z)$ is the amplitude of the electric field at the cutoff surface. It is a constant in a 1D model while it is modified by the reflected surface in a 2D model. $E_{x_0}(z) = \cos(2\arctan(d\phi/dz))$ is used in this simulation. The second term e^{-z^2/w^2} denotes the Gaussian incident beam, and w is the 1/e fold of the Gaussian beam intensity. The third term $e^{ik_0 z^2/\rho}$ comes from the curvature effects of the cutoff surface and the incident wave front. ρ is the effective curvature radius. The curvature effect becomes prominent at the inner reflection. The forth term $e^{i\phi}$ represents the phase modulation by density fluctuation.

The phase of the incident wave is calculated in the 1D geometrical optics as:

$$\phi = 2k_0 \int_{x_0}^{x_{cut}} \epsilon^{1/2}\, dx \quad (4)$$

where ϵ is plasma permittivity which is a function of plasma density and magnetic field (X-mode). A

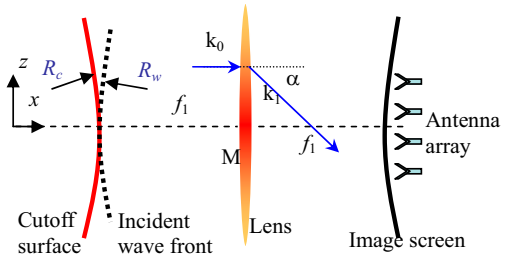

Fig. 1 The model of the reflectometer imaging system.

poloidal plasma density fluctuation causes a phase modulation with poloidal wavenumber k_p. Assume the fluctuation is localized near the cutoff surface and the fluctuation radius is much smaller than the cutoff radius, the cutoff surface is given as:

$$R(x,z) = x^2/R_0 + (z - z_0)^2/R_0 + \sum_j a_j \sin(k_{p_j}(\sigma_j) z + \theta_j) \quad (5)$$

where a is the fluctuation amplitude, the wavenumber k_{p_j} has the standard deviation σ_j, θ_j represents the initial phase, z_0 is the vertical shift of the cutoff surface, and R_0 is the cutoff radius without fluctuation.

In general, the concave mirror is used in the MIR optics system. The role of the concave mirror is similar to the convex lens, which can make a convergent beam. Therefore, the mirror system in MIR can be reduced. Figure 1 shows the schematic diagrams of MIR. The image of the cutoff surface at the detector screen is made by the optical lens M. The wave propagation direction rotates angle α by the optical lens M. The electric field changes as:

$$E(x,z) = E_M(x,z) e^{-i\alpha} = E_M(x,z) e^{-i0.5k_0 z^2/\sqrt{f_1^2 + z^2}} \quad (6)$$

where $E_M(x,z)$ is the electric field at the optical lens M and f_1 is the focal length. If the focal length is infinite, the mirror is reduced to a plane mirror.

The wide aperture lens is necessary to obtain a definitional image. Small optical lens may lose some of the reflected beam and reduce the imaging depth. Practically, the lens size should be at least 2 times larger than the image size. On the other hand, the solution of the electric field in this model is based on the WKB approximation which requires the fluctuations should be in the condition $k < k_0(k_0 L_\epsilon)^{1/3}$, where L_ϵ is the scale length of the plasma permittivity: $L_\epsilon = 1/(d\epsilon/dx)|_{x=x_{cut}}$ [1].

2.2 Numerical results

The amplitude modulation of the reflected wave is mainly caused by the perpendicular (azimuthal) fluctuation. To obtain a large amplitude modification, we assume that the fluctuation amplitude is $a = \lambda_0$, where λ_0 is the wavelength of the incident wave. Figure 2(a) shows the contour plot of the amplitude of electric field in the imaging system. Here, we assume the cutoff surface is at $x = 40$ cm. The launching beam with the frequency of 20 GHz and the beam width of 20 cm is plane wave. The beam is reflected and modified by the cutoff surface. An aperture with a diameter of 30 cm is set at $x = 67$ cm. The optical lens with a focal length of 50 cm is arranged at $x = 140$ cm. Therefore, the inverse image is made at $x = 240$ cm according to the principle of geometrical optics. We assume the poloidal wavenumber is

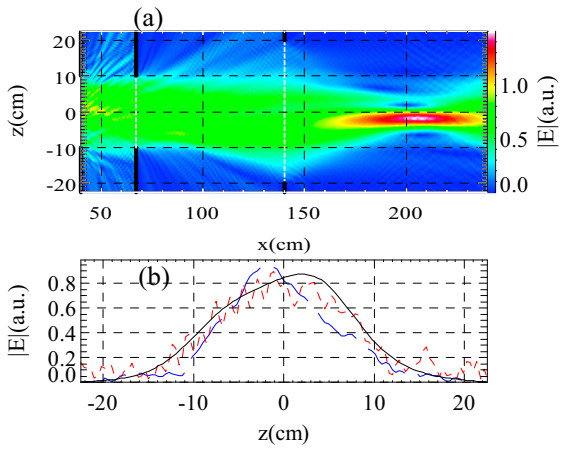

Fig. 2 (a) The contour plot of the electric field intensity in the imaging system. (b) The electric field amplitude profiles at $x = 40$ cm (solid line), $x = 66$ cm (dashed line) and $x = 240$ cm (long dashed line).

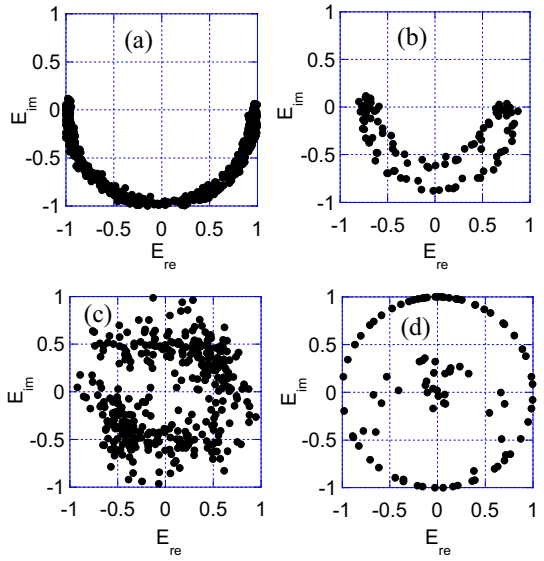

Fig. 3 The complex plots of the reflected waves with $\widetilde{\phi} = 1.0\pi$ at (a) in-focus, (b) weak-focus, (c) out-of-focus conditions, and (d) in-focus of $\widetilde{\phi} = 6.0\pi$.

$k_p = 0.2$ cm^{-1} with the deviation of 0.1 cm^{-1}. The interference pattern is observed outside of the cutoff surface. The beam becomes convergent when it passes through the optical lens, and the image of the cutoff surface is made at the image plane. Figure 2(b) shows the amplitude distributions of the electric field at $x = 40$ cm (solid line), $x = 66$ cm (dashed line) and $x = 240$ cm (long dashed line). The peak of the electric field amplitude in cutoff plane is at $z = 2$ cm while it is at $z = -2$ cm in the image plane, which match the principle of optics imaging. The profile of the electric field amplitude at $x = 66$ cm shows large fluctuation. Therefore, the reflected wave is deformed away from the image plane.

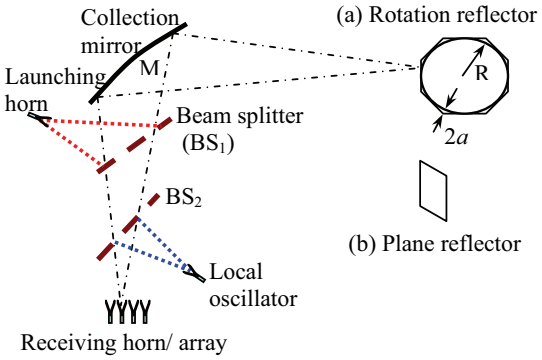

Fig. 4 Schematic view of the laboratory arrangement

The phase modulation of the reflected wave is mainly produced by the radial fluctuations of the cutoff layer. Figure 3 plots the complex amplitude of the reflected waves at (a) in-focus, (b) weak-focus and (c) out-of-focus conditions of the fluctuation amplitude $\lambda_0/4$, and at the (d) in-focus of fluctuation amplitude $3\lambda_0/2$. Therefore, the phase fluctuations in the radial direction are $\widetilde{\phi} = 1.0\pi$ and $\widetilde{\phi} = 6.0\pi$ due to the beam illuminating back and forth. The other parameters are the same as those in figure 2. In the case of weak fluctuation, the Lissajous' plot is a half circle at the in-focus condition. When the focus becomes weak, the Lissajous' plot changes to moon shape. At the out-of-focus condition, the Lissajous' plot exhibits large and random fluctuations. In the case of strong fluctuation, the Lissajous' plot shows deformed circles at the in-focus position. Therefore, the phase is distorted at strong fluctuation.

3. Laboratory test of MIR

3.1 Arrangement of MIR system

Figure 4 shows the Schematic view of the test MIR equipment. It consists of optical elements (i.e., mirrors, lenses, beam splitters and antennas) and a 2D receiver system. The radiofrequency (RF) wave illuminating from the horn antenna is reflected by first beam splitter (BS_1), and comes to the main mirror (M). The main mirror, which is an elliptic concave mirror with the size of 50 cm in diameter, makes a parallel illumination beam to the reflector. The plane and rotation reflectors are used. The plane reflector moves back and forth in experiments. The rotation reflector is made by a thick wood disk with a sinusoid corrugation with wavelength k_θ and depth $2a$. The disk covers with the aluminum foil. The disk is driven by an electric motor in experiments. The reflected wave is collected by the collection mirror (M) and is separated from the illumination beam by the first beam splitter (BS_1). The local oscillation (LO) wave and the reflected wave are mixed at the second beam splitter (BS_2). The beam is focused at the an-

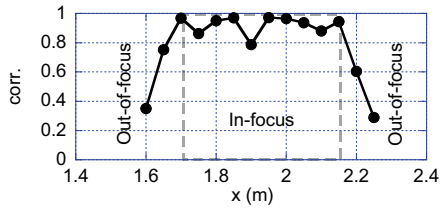

Fig. 5 The in-focus region of the MIR setup.

tenna plane. Therefore, an image of the plasma fluctuation is made. A new pyramidal 2D antenna with a wide band frequency response array is developed. The detail discussions about the antenna array are discussed by Kuwahara [13].

The launching microwave frequency is 48 GHz. The LO wave with the frequency of 48.11 GHz is made by mixing the RF wave (48 GHz) and the lower frequency wave (110 MHz) at an up-converter. By mixing the reflected wave and the LO wave, the 2-D mixer array makes intermediate frequency (IF) signal of 110 MHz. This IF signal contains the amplitude A and the phase ϕ of the density fluctuation in plasma. Here, the phase ϕ indicates the vibrational motion of the reflection layer, and the amplitude A represents the reflected power. The amplitude is obtained by rectifying the IF signal with a diode detector. The phase is obtained by comparing the IF frequency and the mixed signal by the IQ demodulator. I and Q signals correspond to in-phase signal ($I = A\cos(\phi)$) and quadrature signal ($Q = A\sin(\phi)$), respectively.

3.2 Calibration

To obtain an in-focus image of the reflector, the detector array should be arranged at the image plane. The position of the detector array can be calculated by the principle of geometrical optics. The in-focus image is obtained when the reflector is set at about 2 m away from the collection mirror (M) at present setup. Figure 5 shows the cross-correlation of the reflected signals as a function of the distance between the reflector and the collection mirror. The cross-correlation is calculated by the two signals with the distance of 1 cm in the horizontal direction. Here, the plane reflector is used. The cross-correlation is high when the reflector is located at the region between 1.7 m to 2.15 m. This is the in-focus region which agrees with the geometrical optical estimation. Note that the cross-correlation is not exactly one at the in-focus region. It is caused by either the misalignment of the reflector or the optical abbreviation of the MIR system. This problem can be solved by carefully adjusting the optical system. The low correlation at x $>$ 2.2 m and x $<$ 1.6 m means out-of-focus condition in MIR system which may cause the phase and amplitude distortions.

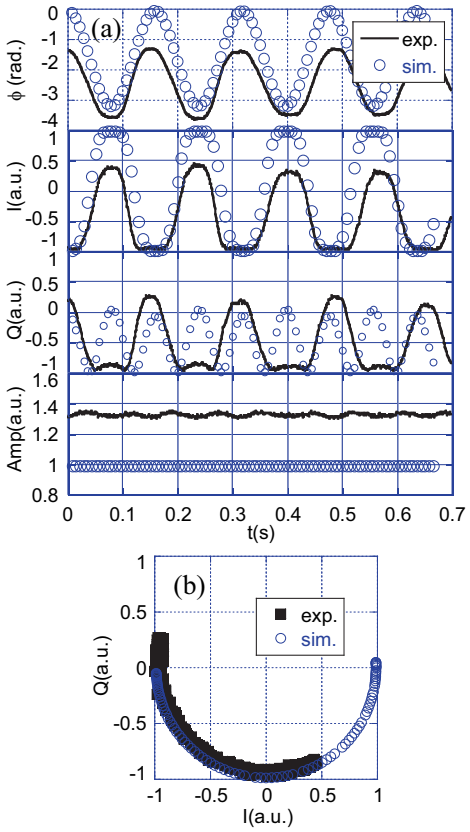

Fig. 6 Waveforms obtained by the plane reflector with phase fluctuation $\widetilde{\phi} = 0.7\pi$ and the simulation with phase fluctuation $\widetilde{\phi} = 1.0\pi$. (a) The phase, I, Q and amplitude from top to bottom, (b) the Lissajous' curves of test and simulation.

3.3 Plane reflector

Measurements are taken with a series of fluctuations when the reflector is arranged at the in-focus region. Figure 6 shows the waveforms in the case of weak fluctuation by using the plane reflector. The phase is obtained from the I and Q signals. The phase fluctuation is about $\widetilde{\phi} = 0.7\pi$ when the plane reflector moves back and forth with the fluctuation amplitude of 1.1 mm along the x direction. Simulation with the phase fluctuation of $\widetilde{\phi} = 1.0\pi$ is also given in this picture. The signals look quite similar although they have different initial phases. The phase fluctuation is quasi-sinusoid which reflects the cutoff surface moves back and forth. The reflected amplitude is modified while it is constant in the simulation. According to the 1D/2D reflectometer model, the fluctuation in the x (radial) direction can only cause the phase fluctuation, not the amplitude fluctuation. In this test, the amplitude fluctuation is small, and it might be caused by the misalignment of the plane reflector. The plane reflector didn't move along the x direction exactly. The Lissajous' curve shows a circular arc with the angle of 0.7π. Therefore, the movement of the cutoff surface in radial direction is reproduced by MIR system.

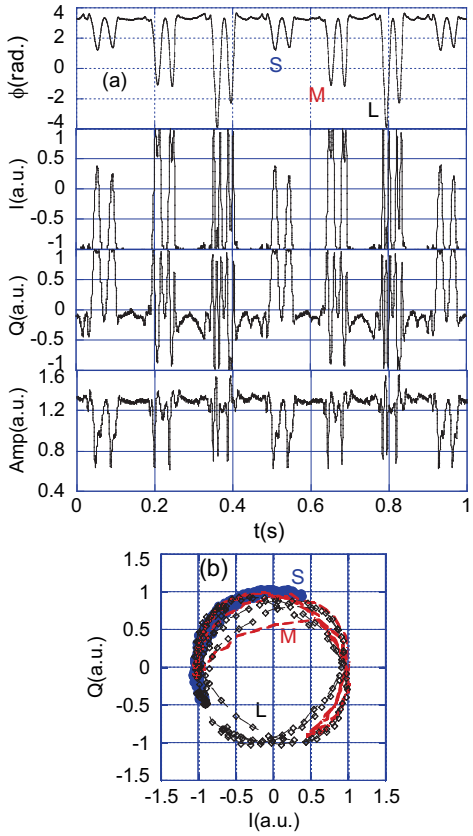

Fig. 7 Waveforms obtained by the rotation reflector. (a) the phase, I, Q and amplitude from top to bottom, (b) the lissajous' curve of the reflected signal.

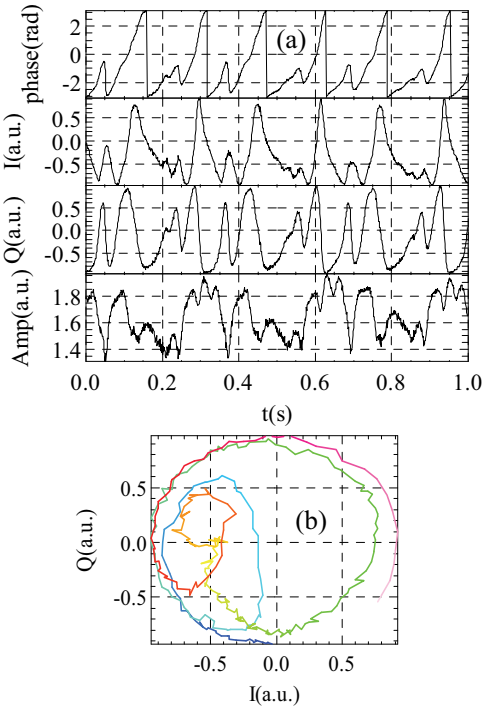

Fig. 8 Waveforms in the strong fluctuations ($\widetilde{\phi} = 6.4\pi$, $k = 0.55$ cm^{-1}). (a) the phase, I, Q and reflected amplitude from top to bottom, (b) the lissajous' curve of the reflected signal.

3.4 Rotation reflector

Figure 7 shows the waveforms obtained by the rotation reflector whose surface is corrugated with three amplitude modulations. The waves are indicated by S, M and L in figure 7(a). Here, the S, M and L represent the small ($\widetilde{\phi} = 2/3\pi$), medial ($\widetilde{\phi} = 4/3\pi$) and large ($\widetilde{\phi} = 2\pi$) phase fluctuations, respectively. The fluctuation amplitudes of S, M and L are 0.1 cm, 0.2 cm and 0.3 cm on the reflector, respectively. The wavenumbers of the waves are about $k = 0.2$ cm^{-1}. The fluctuation signals appear periodically, and the angular velocity of the reflector is estimated about 14.0 rads^{-1} in this test. In the case of small phase fluctuation, the Lissajous' curve shows a standard circular arc. The reflected amplitude is also modulated which is in consistent with the phase fluctuation. The Lissajous' curve becomes a deformed circular arc in the case of medial phase fluctuation, and the reflected amplitude shows two large sharp peaks with higher frequency fluctuations. The amplitude becomes spurious peaks and the Lissajous' curve shows a deformed circle at the strong phase fluctuation. The amplitude distortion may be caused by the strong interference effect near the reflector surface due to the strong fluctuation or the optical abberation of MIR system. Although the Lissajous' curve is deformed, it seems that the phase fluctuation is not so serious distorted by the strong fluctuation. The phase modulation shows a sinusoidal trace which is similar as the reflector surface. It agrees with the longer correlation length measured by IQ detectors in reflectometer [2, 14]. This result suggests that the phase measurement is necessary to obtain the high correlation signals, especially for the strong and high k fluctuations.

The phase distortion depends on not only the fluctuation amplitude but also the wave number of the fluctuation. A rotation reflector with 12 sinusoidal corrugations is made. The modulated amplitude of the corrugation is about 1.0 cm. Therefore, the phase fluctuation is about $\widetilde{\phi} = 6.4\pi$, and the wavenumber is about $k = 0.55$ cm^{-1}. The waveforms of phase, IQ and amplitude signals have strong and complicated fluctuations shown in figure 8. The Lissajous' plot shows circles with deformed circles. The phase rapidly increases when the reflected amplitude becomes large. The phase stops at small reflected amplitude, leading to the runaway-phase phenomenon which is known in standard reflectometry [11]. One possible reason of the runaway-phase phenomenon is that the cutoff surface reflects the launching beam out of the optical lens when the deviation angle of the cutoff surface is too big, leading to small reflected power at the detector surface. The auto-gain amplifier in the phase detector

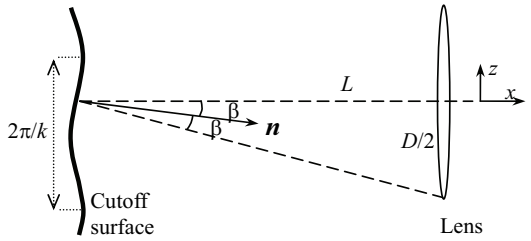

Fig. 9 Schematic illustration of the beam diffraction

doesn't work well with small signals. Another reason might be the strong fluctuations may cause a complicated interference pattern near the reflected surface, MIR can't restore the strong fluctuations, and the interference signals are obtained. Therefore, MIR fails to make the clear image in the strong fluctuations.

4. Summary and discussions

In summary, the numerical study of the 2D fluctuations in MIR system based on the Huygens-Fresnel equation is carried out to simulate the wave propagation. The optical lens is considered in this model. The fluctuation of the cutoff surface is obtained from the phase of the reflected waves when the MIR system arranges at the in-focus condition. A laboratory arrangement of the MIR system is made. The preliminary tests show that the focus of optics in MIR system is one of the key issues to obtain a definitional reflected image. The MIR system works well at the in-focus condition when the fluctuation amplitude is much smaller than the wavelength of the launching wave. The Lissajous' curves from both simulation and experiments have a circular arc shape when MIR works at the in-focus condition. However, the reflected signals are distorted and the phase is lost at strong fluctuations.

This simulation considers the optical lens in the wave equation at the laboratory scenario. It can be used to calibrate the optics and explain the experimental signals. In the present imaging system, the incident beam is perpendicular to the cutoff surface if the optical system is well designed and arranged. Therefore, the refractive effect is not so serious as expected in the plasma. The approximation in this work might be used for the O-mode plasma. However, it is not true under the most conditions. The full wave equation simulation should be used for the actual plasma test because of the strong diffractive effect. Several similar works have been carried out [8–10]. Even so, the phase distortion is still a crucial problem for MIR.

The phase distortion can be estimated from the optical arrangement in MIR system. Figure 9 shows the schematic illustration of the beam diffraction in MIR system. Where, $\boldsymbol{n}$ is the surface normal and β is the cutting angle of the cutoff surface. D is the diameter of the optical lens. L is the distance between the optical lens and the reflector surface. The parallel launching beam is deflected an angle 2β by the reflector surface. The phase lost will happen when the lens can't collect the main reflected beam. If we assume the modulated wave is sinusoid and $L >> D$, the relationship between the fluctuation amplitude a and the wavenumber k is given as

$$ak < \frac{D}{4L} \tag{7}$$

for the in-focus imaging. The phase lost happens when the fluctuation amplitude is much larger than $D/(4kL)$. As shown in figure 7 (b), the wavenumber k of the modulated wave is estimated about 0.2 cm^{-1}. Therefore, the fluctuation amplitude should be smaller than 0.16 cm for the phase fluctuation without distortion. In the case of small fluctuation, the fluctuation amplitudes is about 0.1 cm, so the circular IQ signals are obtained. In the case of medial and large fluctuations, the fluctuation amplitudes are 0.2 cm and 0.3 cm, respectively. So the IQ signals are distorted. Therfore, MIR can't obtain the clear image of the large amplitude fluctuations with $a \gg D/(4kL)$ due to the diffraction effect of the reflected wave.

Acknowledgements

This work is carried out as one of the NINS Imaging Science Project (Grant No. NIFS08KEIN0021). This work is also supported by NIFS (Grant No. NIFS08ULPP525), and SOKENDAI (Grant No. NIFS08GLPP003).

References

[1] E. Mazzucato, Rev. Sci. Instrum. **69**, 2201 (1998).
[2] T. Estrada, et al., Phys. Plasmas **8**, 2657 (2001).
[3] R. Sabot, et al., Plasma Phys. Control. Fusion **48**, B421 (2006)
[4] H. Park, et al., Rev. Sci. Instrum. **74**, 4239 (2003).
[5] G.D. Conway, et al., Nucl. Fusion **46**, S665 (2006)
[6] A. Ejiri, et al., Plasma Phys. Control. Fusion **50**, 065003 (2008)
[7] S. Yamaguchi, et al., Rev. Sci. Instrum. **77**, 10E930 (2006).
[8] T. Munsat, et al., Plasma Phys. Control. Fusion **45**, 469 (2003)
[9] G.J. Kramer, et al., Plasma Phys. Control. Fusion **46**, 695 (2004)
[10] M. Ignatenko, et al., Nucl. Fusion **46**, S760 (2006)
[11] E. Mazzucato, et al., Phys. Plasmas **9**, 1955 (2002).
[12] Y. Lin, et al., Plasma Phys. Control. Fusion **43**, L1 (2001)
[13] D. Kuwahara, et al., Development of 2D antenna array for MIR in LHD, International Congress on Plasma Physics, Kyushu Japan, 2008
[14] J. Schirmer, et al., Plasma Phys. Control. Fusion **49**, 1019 (2007)